

Spacelike Lines with Special Trajectories and Invariant Axodes

Areej A. Almoneef ¹  and Rashad A. Abdel-Baky ^{2,*}

¹ Department of Mathematical Sciences, College of Science, Princess Nourah bint Abdulrahman University, P.O. Box 84428, Riyadh 11671, Saudi Arabia

² Department of Mathematics, Faculty of Science, University of Assiut, Assiut 71516, Egypt

* Correspondence: rbaky@live.com

Abstract: The association between the instantaneous invariants of a one-parameter Lorentzian spatial movement and the spacelike lines with certain trajectories is considered in this study. To be more precise, we present a theoretical formulation of a Lorentzian inflection line congruence, which is the spatial symmetrical of the inflection circle of planar kinematics. Finally, we establish novel Lorentzian explanations for the Disteli and Euler–Savary formulae. Our results add to a better understanding of the interaction between axodes and Lorentzian spatial movements, with potential implications in fields such as robotics and mechanical engineering.

Keywords: timelike axodes; Euler–Savary equation; Disteli-axis

MSC: 53A04; 53A05; 53A17

1. Introduction

Differential line geometry is the study of line families in three-dimensional space. The ambient space may or may not be Euclidean. Motivating differential line geometry is its extensive use in robot kinematics and mechanism design, as a result of its direct relationship to spatial movement (kinematics). In spatial movements, however, it is necessary to examine the intrinsic properties of the line trajectory in view of the ruled surfaces. In addition, the instantaneous screw axis \mathbb{ISA} of a movable body is widely known to trace a set of two ruled surfaces known as the stationary axode and the movable axode, with \mathbb{ISA} as their ruling (creating) in the stationary space and the movable space, respectively. The axodes roll and slide with regard to one another during the movement, ensuring that tangential contact between the axodes is maintained along the entire length of the two matting rulings (one in each axode), which determine the \mathbb{ISA} at any given moment. A specific movement is thought to give rise to a distinct family of axodes, and the opposite is also true. If the axodes of any movement are defined, then the movement can be recreated without identifying the mechanism's physical components, their configuration, private dimensions, or the relationship between them. In the operations of synthesis, the investigation has revealed that axodes are the middle of the physical mechanism and the actual movement of their constituents [1–4]. One of the best effective techniques for analyzing the movement of line space appears to reveal a relationship between this space and dual numbers. W. Clifford first discussed dual numbers after him. E. Study used it as a tool for understanding differential line geometry and kinematics. He gave special attention to the representation of straight lines by dual unit vectors and demonstrated their well-known mapping (E. Study map). The line families of the three-dimensional Euclidean space \mathbb{E}^3 are acted upon by the points on the dual unit sphere of the three-dimensional dual space \mathbb{D}^3 [5–13]. In the three-dimensional Minkowski space \mathbb{E}_1^3 , the Lorentzian metric can have either a positive, negative, or zero Lorentzian causal character, whereas the metric in the three-dimensional Euclidean space \mathbb{E}^3 are always positive definite. Consequently, the kinematic and geometric clarifications can be made more relevant in \mathbb{E}_1^3 (see [14–17]). Some papers provide us with additional inspiration for our work (see [18–35]).



Citation: Almoneef, A.A.; Abdel-Baky, R.A. Spacelike Lines with Special Trajectories and Invariant Axodes. *Symmetry* **2023**, *15*, 1087. <https://doi.org/10.3390/sym15051087>

Academic Editor: Alexei Kanel-Belov

Received: 4 April 2023

Revised: 25 April 2023

Accepted: 10 May 2023

Published: 15 May 2023



Copyright: © 2023 by the authors. Licensee MDPI, Basel, Switzerland. This article is an open access article distributed under the terms and conditions of the Creative Commons Attribution (CC BY) license (<https://creativecommons.org/licenses/by/4.0/>).

In this work, we employ the dual vector calculus established by E. Study in their investigations of geometry. The curvature functions of a spacelike line are constructed from the axodes' invariants. Similar to the kinematic theory of planar and spherical movement, the well-known inflection circle is determined on the Lorentzian dual unit sphere. Using E. Study's map, a Lorentzian line congruence is then introduced and its spatial equivalent is examined. The acquired expressions degenerate into a quadratic form that provides a clear understanding of the geometric properties of the Lorentzian inflection line congruence. Moreover, the invariants of the axodes are used to derive new Lorentzian proofs of the Euler–Savary and Disteli formulae.

2. Preliminaries

An overview of the dual numbers theory and dual Lorentzian vectors is provided in this Section [1–5,36–38]. The formula: $\hat{\zeta} = \zeta + \varepsilon\zeta^*$ is known as the dual number such that $\varepsilon \neq 0$, and $\varepsilon^2 = 0$, where ζ , and ζ^* are real numbers. This is actually very similar to the concept of a complex number, the main distinction being that in a complex number $\varepsilon^2 = -1$. Then, the set

$$\mathbb{D}^3 = \{\hat{\zeta} := \zeta + \varepsilon\zeta^* = (\hat{\zeta}_1, \hat{\zeta}_2, \hat{\zeta}_3)\},$$

together with the Lorentzian metric

$$\langle \hat{\zeta}, \hat{\zeta} \rangle = -\hat{\zeta}_1^2 + \hat{\zeta}_2^2 + \hat{\zeta}_3^2,$$

is named Lorentzian 3-space \mathbb{D}_1^3 . A dual vector $\hat{\zeta} \in \mathbb{D}_1^3$ is a spacelike dual if $\langle \hat{\zeta}, \hat{\zeta} \rangle > 0$ or $\hat{\zeta} = \mathbf{0}$, a timelike dual if $\langle \hat{\zeta}, \hat{\zeta} \rangle < 0$, and a lightlike or null dual if $\langle \hat{\zeta}, \hat{\zeta} \rangle = 0$ and $\hat{\zeta} \neq \mathbf{0}$. If $\zeta \neq \mathbf{0}$ the norm of $\hat{\zeta}$ is specified by

$$\|\hat{\zeta}\| = \sqrt{|\langle \hat{\zeta}, \hat{\zeta} \rangle|} = \|\zeta\| \left(1 + \varepsilon \frac{\langle \zeta, \zeta^* \rangle}{\|\zeta\|^2}\right).$$

As a result, the vector $\hat{\zeta}$ is known as a spacelike (timelike) dual unit vector if $\|\hat{\zeta}\|^2 = 1$ ($\|\hat{\zeta}\|^2 = -1$). Then,

$$\|\hat{\zeta}\|^2 = \pm 1 \iff \|\zeta\|^2 = \pm 1, \langle \zeta, \zeta^* \rangle = 0. \quad (1)$$

The six components ζ_i , and ζ_i^* ($i = 1, 2, 3$) of ζ , and ζ^* are known as the normed Plücker coordinates. For any two dual vectors $\hat{\zeta} = (\hat{\zeta}_1, \hat{\zeta}_2, \hat{\zeta}_3)$ and $\hat{\xi} = (\hat{\xi}_1, \hat{\xi}_2, \hat{\xi}_3)$ of \mathbb{D}_1^3 , the vector product is specified by

$$\hat{\zeta} \times \hat{\xi} = \begin{vmatrix} -\hat{\mathbf{e}}_1 & \hat{\mathbf{e}}_2 & \hat{\mathbf{e}}_3 \\ \hat{\zeta}_1 & \hat{\zeta}_2 & \hat{\zeta}_3 \\ \hat{\xi}_1 & \hat{\xi}_2 & \hat{\xi}_3 \end{vmatrix},$$

where $\hat{\mathbf{e}}_1, \hat{\mathbf{e}}_2, \hat{\mathbf{e}}_3$ is the canonical dual basis of \mathbb{D}_1^3 . The hyperbolic and Lorentzian (de Sitter space) dual unit spheres, respectively, are:

$$\mathbb{H}_+^2 = \{\hat{\zeta} \in \mathbb{D}_1^3 \mid \|\zeta\|^2 := -\hat{\zeta}_1^2 + \hat{\zeta}_2^2 + \hat{\zeta}_3^2 = -1\},$$

and

$$\mathbb{S}_1^2 = \{\hat{\zeta} \in \mathbb{D}_1^3 \mid \|\zeta\|^2 := -\hat{\zeta}_1^2 + \hat{\zeta}_2^2 + \hat{\zeta}_3^2 = 1\},$$

respectively. Then we can state the E. Study map as the ring-shaped hyperboloid image of spacelike lines, the common asymptotic cone image of null-lines, and the oval shaped hyperboloid image of timelike lines (see Figure 1).

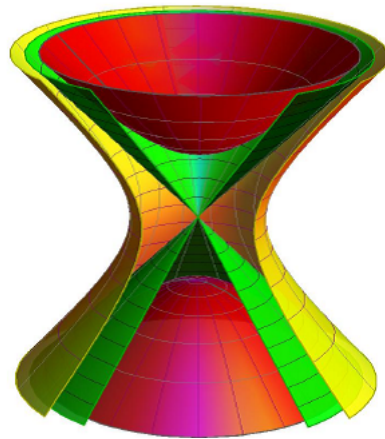


Figure 1. The dual hyperbolic and dual Lorentzian unit spheres.

Via the E. Study map, a timelike ruled surface (\hat{x}) in Minkowski 3-space \mathbb{E}_1^3 is represented by a regular curve $t \in \mathbb{R} \mapsto \hat{x}(t) \in \mathbb{H}_+^2$. Similarly, a regular curve $t \in \mathbb{R} \mapsto \hat{x}(t) \in \mathbb{S}_1^2$ shows a spacelike or timelike ruled surface in \mathbb{E}_1^3 . $\hat{x}(t)$ are specified with the rulings of the surface and we will not distinguish between ruled surfaces and their explaining dual curves from now on.

Definition 1. For any two (non-null) dual vectors $\hat{\zeta}$ and $\hat{\xi}$ in \mathbb{D}_1^3 , we have [15–17]:

- (a) If $\hat{\zeta}$ and $\hat{\xi}$ are two dual spacelike vectors, then
- There exists a single dual number $\hat{\theta} = \theta + \varepsilon\theta^*$; $0 \leq \theta \leq \pi$, and $\theta^* \in \mathbb{R}$ such that $\langle \hat{\zeta}, \hat{\xi} \rangle = \|\hat{\zeta}\| \|\hat{\xi}\| \cos \hat{\theta}$; if $\hat{\zeta}$ and $\hat{\xi}$ span a dual spacelike plane. This number corresponds to the dual angle between $\hat{\zeta}$ and $\hat{\xi}$.
 - There exists a single dual number $\hat{\theta} = \theta + \varepsilon\theta^* \geq 0$ such that $\langle \hat{\zeta}, \hat{\xi} \rangle = \varepsilon \|\hat{\zeta}\| \|\hat{\xi}\| \cosh \hat{\theta}$, where $\varepsilon = +1$ or $\varepsilon = -1$ via $\text{sign}(\hat{\zeta}_2) = \text{sign}(\hat{\xi}_2)$ or $\text{sign}(\hat{\zeta}_2) \neq \text{sign}(\hat{\xi}_2)$, respectively, if $\hat{\zeta}$ and $\hat{\xi}$ span a dual timelike plane. This number corresponds to the central dual angle between $\hat{\zeta}$ and $\hat{\xi}$.
- (b) If $\hat{\zeta}$ and $\hat{\xi}$ are two dual timelike vectors, then there exists a single dual number $\hat{\theta} = \theta + \varepsilon\theta^* \geq 0$ such that $\langle \hat{\zeta}, \hat{\xi} \rangle = \varepsilon \|\hat{\zeta}\| \|\hat{\xi}\| \cosh \hat{\theta}$, where $\varepsilon = -1$ or $\varepsilon = +1$ via $\hat{\zeta}$ and $\hat{\xi}$ have the same time-direction or different time-direction, respectively. This dual number is named the Lorentzian timelike dual angle between $\hat{\zeta}$ and $\hat{\xi}$.
- (c) If $\hat{\zeta}$ is dual spacelike, and $\hat{\xi}$ is dual timelike, then there exists a single dual number $\hat{\theta} = \theta + \varepsilon\theta^* \geq 0$ such that $\langle \hat{\zeta}, \hat{\xi} \rangle = \varepsilon \|\hat{\zeta}\| \|\hat{\xi}\| \sinh \hat{\theta}$, where $\varepsilon = +1$ or $\varepsilon = -1$ via $\text{sign}(\hat{\zeta}_2) = \text{sign}(\hat{\xi}_1)$ or $\text{sign}(\hat{\zeta}_2) \neq \text{sign}(\hat{\xi}_1)$. This number is called the Lorentzian timelike dual angle between $\hat{\zeta}$ and $\hat{\xi}$.

One-Parameter Lorentzian Dual Spherical Movements

Assume that \mathbb{S}_{1m}^2 and \mathbb{S}_{1f}^2 are two Lorentzian dual unit spheres with \hat{o} as a mutual center in \mathbb{D}_1^3 . Suppose $\{\hat{\zeta}\} = \{\hat{o}; \hat{\zeta}_1(\text{timelike}), \hat{\zeta}_2, \hat{\zeta}_3\}$, and $\{\hat{e}\} = \{\hat{o}; \hat{e}_1(\text{timelike}), \hat{e}_2, \hat{e}_3\}$ are two orthonormal dual frames of \mathbb{S}_{1m}^2 and \mathbb{S}_{1f}^2 , respectively. When setting $\{\hat{\zeta}\}$ stationary, the elements of $\{\hat{e}\}$ are functions of a real parameter $t \in \mathbb{R}$ (say the time). Therefore, \mathbb{S}_{1m}^2 moves against \mathbb{S}_{1f}^2 . This movement is known as a one-parameter Lorentzian dual spherical movement and it is denoted by $\mathbb{S}_{1m}^2/\mathbb{S}_{1f}^2$. Via the E. Study map, if \mathbb{S}_{1m}^2 and \mathbb{S}_{1f}^2 are matching the Lorentzian line spaces \mathbb{L}_m (movable) and \mathbb{L}_f (stationary), respectively, then $\mathbb{S}_{1m}^2/\mathbb{S}_{1f}^2$ demonstrates the one-parameter Lorentzian spatial movement $\mathbb{L}_m/\mathbb{L}_f$ in \mathbb{E}_1^3 .

By the 1st order instantaneous features of $\mathbb{L}_m/\mathbb{L}_f$, consider a Lorentzian dual unit sphere \mathbb{S}_{1r}^2 heading by $\{\widehat{\mathbf{r}}\} = \{\widehat{\mathbf{s}}; \widehat{\mathbf{r}}_1(\text{timelike}), \widehat{\mathbf{r}}_2, \widehat{\mathbf{r}}_3\}$ as follows: $\widehat{\mathbf{r}}_1(t) = \mathbf{r}_1(t) + \varepsilon\mathbf{r}_1^*(t)$ is the instantaneous screw axis (ISSA) for the movement $\mathbb{L}_m/\mathbb{L}_f$, and $\widehat{\mathbf{r}}_2(t) := \mathbf{r}_2(t) + \varepsilon\mathbf{r}_2^*(t) = \frac{d\mathbf{r}_1}{dt} \left\| \frac{d\mathbf{r}_1}{dt} \right\|^{-1}$ as the mutual spacelike central normal of two separated screw axes. $\widehat{\mathbf{r}}_3(t) = \widehat{\mathbf{r}}_1 \times \widehat{\mathbf{r}}_2$ represents a third spacelike dual unit vector. The set $\{\mathbf{r}\}$, located as such, will be named induce Blaschke frame. It is fully specified by the 1st order ownerships of the movement.

According to the E. Study map, we have two timelike ruled surfaces created by the ISSA. One is in the stationary Lorentzian space \mathbb{L}_f and another in the movable Lorentzian space \mathbb{L}_m . The first timelike ruled surface is named stationary axode π_f , whereas the second one is named movable axode π_m . These two axodes have all the times, a mutual tangent along the ISSA, and they slide on each other. The origin \mathbf{s} is the mutual central point established by the ISSA of the movement $\mathbb{L}_m/\mathbb{L}_f$ between the movable axode π_m in \mathbb{L}_m and stationary axode π_f in \mathbb{L}_f . Then,

$$\widehat{\mathbf{r}}_1 \times \widehat{\mathbf{r}}_2 = \widehat{\mathbf{r}}_3, \widehat{\mathbf{r}}_1 \times \widehat{\mathbf{r}}_3 = -\widehat{\mathbf{r}}_2, \widehat{\mathbf{r}}_2 \times \widehat{\mathbf{r}}_3 = -\widehat{\mathbf{r}}_1. \tag{2}$$

The dual arc length $d\widehat{s}_i = ds_i + \varepsilon ds_i^*$ ($i = m, f$) of the axodes is $d\widehat{s}_i = \left\| \frac{d\mathbf{r}_1}{dt} \right\| dt = \widehat{p} dt$. Since $\widehat{p} = p + \varepsilon p^*$ contains only 1st order derivatives of $\widehat{\xi}_1(t)$, it is a 1st order property of $\mathbb{L}_m/\mathbb{L}_f$, especially with its dual speed. Put $d\widehat{s} = ds + \varepsilon ds^*$ to symbolize $d\widehat{s}_i$, since they are equal to each other. The mutual distribution parameter of π_i is

$$\mu(s) := \frac{ds^*}{ds} = \frac{p^*}{p}. \tag{3}$$

Proposition 1. *Through the movement $\mathbb{L}_m/\mathbb{L}_f$, the movable timelike axode osculates with the stationary timelike axode on the timelike ISSA in the 1st order at any instant t (compared with [6–8]).*

From now on, we will frequently omit the explicit \widehat{s} from our computations. If dash is the derivative with respect to \widehat{s} , then therefore the Blaschke formulae are

$$\begin{pmatrix} \widehat{\mathbf{r}}_1' \\ \widehat{\mathbf{r}}_2' \\ \widehat{\mathbf{r}}_3' \end{pmatrix} \Big|_i = \begin{pmatrix} 0 & 1 & 0 \\ 1 & 0 & \widehat{\gamma}_i \\ 0 & -\widehat{\gamma}_i & 0 \end{pmatrix} \begin{pmatrix} \widehat{\mathbf{r}}_1 \\ \widehat{\mathbf{r}}_2 \\ \widehat{\mathbf{r}}_3 \end{pmatrix} = \widehat{\omega}_i \times \begin{pmatrix} \widehat{\mathbf{r}}_1 \\ \widehat{\mathbf{r}}_2 \\ \widehat{\mathbf{r}}_3 \end{pmatrix}, \tag{4}$$

where

$$\widehat{\gamma}_i = \gamma_i + \varepsilon(\Gamma_i - \mu\gamma_i) = \det(\widehat{\mathbf{r}}_1, \widehat{\mathbf{r}}_1', \widehat{\mathbf{r}}_1''), \tag{5}$$

are the dual geodesic curvatures of the axodes π_i , and $\widehat{\omega}_i := \omega_i + \varepsilon\omega_i^* = \widehat{\gamma}_i\widehat{\mathbf{r}}_1 - \widehat{\mathbf{r}}_3$, is the Darboux vector. The tangent vector of the striction curve $\mathbf{s}(s)$ is

$$\frac{d\mathbf{s}}{ds} \Big|_i = -\Gamma_i\mathbf{r}_1 + \mu\mathbf{r}_1. \tag{6}$$

The functions $\gamma_i(s)$, $\Gamma_i(s)$, and $\mu(s)$ are referred as the curvature (construction) functions of the timelike axodes. Under the hypothesis that $|\widehat{\gamma}_i| < 1$, the timelike Disteli-axis (evolute or curvature axis) is

$$\widehat{\mathbf{b}}_i = \mathbf{b}_i + \mathbf{b}_i = \frac{\widehat{\omega}_i}{\|\widehat{\omega}_i\|} = \frac{\widehat{\gamma}_i}{\sqrt{1 - \widehat{\gamma}_i^2}}\widehat{\mathbf{r}}_1 - \frac{1}{\sqrt{1 - \widehat{\gamma}_i^2}}\widehat{\mathbf{r}}_3. \tag{7}$$

Let $\widehat{\phi}_i = \phi_i + \phi_i$ be the radius of curvature among $\widehat{\mathbf{b}}_i$ and $\widehat{\xi}_1$. Then,

$$\widehat{\mathbf{b}}_i = \mathbf{b}_i + \mathbf{b}_i = \sinh \widehat{\phi}_i\widehat{\mathbf{r}}_1 - \cosh \widehat{\phi}_i\widehat{\mathbf{r}}_3, \tag{8}$$

where

$$\widehat{\gamma}_i = \gamma_i + \varepsilon(\Gamma_i - \mu\gamma_i) = \tanh \widehat{\phi}_i. \tag{9}$$

Thus, we attain

$$\tanh \widehat{\phi}_f - \tanh \widehat{\phi}_m = \widehat{\gamma}_f - \widehat{\gamma}_m. \tag{10}$$

Equation (10) is a new Lorentzian dual version of the well-known Euler–Savary formula (compared with [1–8]). This version furnishes a correlation for the two timelike axodes in the movement $\mathbb{L}_m/\mathbb{L}_f$. From the real and dual parts of Equation (10), respectively, we obtain:

$$\tanh \phi_f - \tanh \phi_m = \gamma_f - \gamma_m, \tag{11}$$

and

$$\frac{\phi_m^*}{\cosh^2 \phi_f} - \frac{\phi_f^*}{\cosh^2 \phi_m} + \mu(\tanh \phi_f - \tanh \phi_m) = \Gamma_f - \Gamma_m. \tag{12}$$

Equations (11) and (12) are new Disteli formulae of spatial kinematics for the timelike axode π_i .

Now, assuming that the induce Blaschke frame is stationary in \mathbb{L}_m , then,

$$\mathbb{L}_m/\mathbb{L}_f : \begin{pmatrix} \widehat{\mathbf{r}}_1 \\ \widehat{\mathbf{r}}_2 \\ \widehat{\mathbf{r}}_3 \end{pmatrix} = \begin{pmatrix} 0 & 1 & 0 \\ 1 & 0 & \widehat{\gamma} \\ 0 & -\widehat{\gamma} & 0 \end{pmatrix} \begin{pmatrix} \widehat{\mathbf{r}}_1 \\ \widehat{\mathbf{r}}_2 \\ \widehat{\mathbf{r}}_3 \end{pmatrix} = \widehat{\omega} \times \begin{pmatrix} \widehat{\mathbf{r}}_1 \\ \widehat{\mathbf{r}}_2 \\ \widehat{\mathbf{r}}_3 \end{pmatrix}, \tag{13}$$

where

$$\widehat{\omega} := \widehat{\omega}_f - \widehat{\omega}_m = \omega \widehat{\mathbf{r}}_1, \tag{14}$$

is the induce Darboux vector. $\widehat{\gamma} := \|\widehat{\omega}\| = \omega + \varepsilon\omega^*$ is the induce dual geodesic curvature, where $\gamma := \omega = \gamma_f - \gamma_m$ and $\gamma^* := \omega^* = \Gamma_f - \Gamma_m - \mu(\gamma_f - \gamma_m)$ are the rotational angular speed and translational angular speed of the movement $\mathbb{L}_m/\mathbb{L}_f$. Likewise, they are both kinematic invariants, correspondingly.

Consequently, it is possible to state the following corollary:

Proposition 2. *Through the movement $\mathbb{L}_m/\mathbb{L}_f$, the pitch $h(s)$ of the movement $\mathbb{L}_m/\mathbb{L}_f$ is*

$$h(s) := \frac{\omega^*}{\omega} = \frac{\Gamma_f - \Gamma_m}{\gamma_f - \gamma_m} - \mu. \tag{15}$$

In our treatise, we shall set $\omega^* \neq 0$ to leave out the pure translational movements. Furthermore, zero divisors $\omega = 0$ are eliminated. As a result, we only consider non-torsional movements, and the timelike axodes are non-developable ruled surfaces ($\mu \neq 0$).

3. Spacelike Lines with Special Trajectories

Through the movement $\mathbb{L}_m/\mathbb{L}_f$, in general, any stationary spacelike line related with the movable timelike axode will produce a spacelike or timelike ruled surface, (\widehat{x}) in \mathbb{L}_f . On the assumption that it is a timelike ruled surface, this ruled surface is known as a spacelike line trajectory in kinematics. Given that all kinematic–geometric properties may therefore be determined using the invariants of the timelike axodes of the movement $\mathbb{L}_m/\mathbb{L}_f$. Therefore, we investigate a spacelike dual unit vector \widehat{x} such that its coordinates are

$$\widehat{x} = \widehat{x}^t \boldsymbol{\xi}, \quad \widehat{x} = \begin{pmatrix} \widehat{x}_1 \\ \widehat{x}_2 \\ \widehat{x}_3 \end{pmatrix}, \quad \{\widehat{\mathbf{r}}\} = \begin{pmatrix} \widehat{\mathbf{r}}_1 \\ \widehat{\mathbf{r}}_2 \\ \widehat{\mathbf{r}}_3 \end{pmatrix}, \tag{16}$$

where

$$\begin{aligned} -x_1^2 + x_2^2 + x_3^2 &= 1, \\ -x_1 x_1^* + x_2 x_2^* + x_3 x_3^* &= 0. \end{aligned} \tag{17}$$

The velocity and the acceleration vectors of $\widehat{\mathbf{x}}(\widehat{s})$, respectively, are:

$$\widehat{\mathbf{x}}' := \widehat{\omega} \times \widehat{\mathbf{x}} = \widehat{\omega}(-\widehat{x}_3 \widehat{\mathbf{r}}_2 + \widehat{x}_2 \widehat{\mathbf{r}}_3). \quad (18)$$

and

$$\widehat{\mathbf{x}}'' = -\widehat{x}_3 \widehat{\omega} \widehat{\mathbf{r}}_1 - (\widehat{x}_2 \widehat{\omega}^2 + \widehat{x}_3 \widehat{\omega}') \widehat{\mathbf{r}}_2 + (-\widehat{x}_1 \widehat{\omega} + \widehat{x}_2 \widehat{\omega}' - \widehat{x}_3^2 \widehat{\omega}^2) \widehat{\mathbf{r}}_3. \quad (19)$$

Then,

$$\widehat{\mathbf{x}}' \times \widehat{\mathbf{x}}'' = \widehat{\omega}^2 [(1 + \widehat{x}_1^2) \widehat{\omega}_{,1} - \widehat{x}_3 \widehat{\mathbf{x}}]. \quad (20)$$

In order to examine (\widehat{x}) , the Blaschke frame is specified as:

$$\widehat{\mathbf{x}} = \widehat{\mathbf{x}}(\widehat{s}), \quad \widehat{\mathbf{t}}(\widehat{s}) = \widehat{\mathbf{x}}' \left\| \widehat{\mathbf{x}}' \right\|^{-1}, \quad \widehat{\mathbf{g}}(\widehat{s}) = \widehat{\mathbf{x}} \times \widehat{\mathbf{t}}, \quad (21)$$

where

$$\left. \begin{aligned} \widehat{\mathbf{x}} \times \widehat{\mathbf{t}} &= \widehat{\mathbf{g}}, \quad \widehat{\mathbf{x}} \times \widehat{\mathbf{g}} = -\widehat{\mathbf{t}}, \quad \widehat{\mathbf{t}} \times \widehat{\mathbf{g}} = \widehat{\mathbf{x}}, \\ \langle \widehat{\mathbf{x}}, \widehat{\mathbf{x}} \rangle &= \langle \widehat{\mathbf{t}}, \widehat{\mathbf{t}} \rangle = -\langle \widehat{\mathbf{g}}, \widehat{\mathbf{g}} \rangle = 1. \end{aligned} \right\}$$

Here, $\widehat{\mathbf{x}}$, $\widehat{\mathbf{t}}$, and $\widehat{\mathbf{g}}$ are orthogonal intersected lines at a point \mathbf{c} on $\widehat{\mathbf{x}}$ known as the striction (or central) point. The locus of \mathbf{c} is the striction curve on $(\widehat{x}) \in \mathbb{L}_f$. From Equation (18), the dual arc length $d\widehat{v} = dv + \varepsilon dv^*$ of $\widehat{\mathbf{x}}(\widehat{s})$ is

$$d\widehat{v} = \left\| \widehat{\mathbf{x}}' \right\| d\widehat{s} = \widehat{\omega} \sqrt{1 + \widehat{x}_1^2} d\widehat{s}. \quad (22)$$

Thus,

$$\frac{d}{d\widehat{v}} \begin{pmatrix} \widehat{\mathbf{x}} \\ \widehat{\mathbf{t}} \\ \widehat{\mathbf{g}} \end{pmatrix} = \begin{pmatrix} 0 & 1 & 0 \\ -1 & 0 & \widehat{\chi} \\ 0 & \widehat{\chi} & 0 \end{pmatrix} \begin{pmatrix} \widehat{\mathbf{x}} \\ \widehat{\mathbf{t}} \\ \widehat{\mathbf{g}} \end{pmatrix}, \quad (23)$$

where

$$\widehat{\chi}(\widehat{v}) = \det(\widehat{\mathbf{x}}, \widehat{\mathbf{x}}', \widehat{\mathbf{x}}'') \left\| \widehat{\mathbf{x}}' \right\|^{-3} = \frac{\widehat{\omega} \widehat{x}_1 (\widehat{x}_1^2 + 1) - \widehat{x}_3}{\widehat{\omega} (\widehat{x}_1^2 + 1)^{\frac{3}{2}}}, \quad (24)$$

is the dual spherical curvature of $\widehat{\mathbf{x}}(\widehat{v})$. The tangent direction of $\mathbf{c}(v)$ is:

$$\frac{d\mathbf{c}}{dv} = -\Gamma \mathbf{x}(v) + \mu \mathbf{g}(v), \quad (25)$$

which will be a spacelike (timelike) curve if $|\mu| < |\Gamma|$ ($|\mu| > |\Gamma|$). $\gamma(v)$, $\Gamma(v)$, and $\mu(v)$ are the construction functions of the (\widehat{x}) . Via the assumption that $|\widehat{\chi}| < 1$, the timelike Disteli-axis is:

$$\widehat{\mathbf{b}} = \mathbf{b} + \varepsilon \mathbf{b}^* = \frac{\widehat{\chi}}{\sqrt{1 - \widehat{\chi}^2}} \widehat{\mathbf{x}} - \frac{1}{\sqrt{1 - \widehat{\chi}^2}} \widehat{\mathbf{g}}. \quad (26)$$

Put $\widehat{\phi} = \phi + \varepsilon \phi^*$ as the radius of curvature through $\widehat{\mathbf{b}}$ and $\widehat{\mathbf{x}}$. Then,

$$\widehat{\mathbf{b}} = \sinh \widehat{\phi} \widehat{\mathbf{x}} - \cosh \widehat{\phi} \widehat{\mathbf{g}}, \quad (27)$$

where

$$\widehat{\chi} := \chi + \varepsilon \chi^* = \chi + \varepsilon (\Gamma - \mu \chi) = \tanh \widehat{\phi}. \quad (28)$$

Equations (24) and (28) lead to

$$\tanh \widehat{\phi} = \frac{\widehat{\omega} \widehat{x}_1 (\widehat{x}_1^2 + 1) - \widehat{x}_3}{\widehat{\omega} (\widehat{x}_1^2 + 1)^{\frac{3}{2}}}. \quad (29)$$

Furthermore, we have

$$\left. \begin{aligned} \widehat{\kappa} &:= \kappa + \varepsilon\kappa^* = \|\widehat{x}' \times \widehat{x}''\| \|\widehat{x}'\|^{-3} = \sqrt{1 - \widehat{\chi}^2} = \frac{1}{\cosh^2 \widehat{\varphi}}, \\ \widehat{\tau} &:= \tau + \varepsilon\tau = \det(\widehat{x}', \widehat{x}'', \widehat{x}''') \|\widehat{x}' \times \widehat{x}''\|^{-2} = \pm \frac{\widehat{\chi}'}{1 - \widehat{\chi}^2} = \pm \widehat{\varphi}', \end{aligned} \right\} \quad (30)$$

where $\widehat{\kappa}$ is the dual curvature and $\widehat{\tau}$ is the dual torsion, respectively.

3.1. Plucker Coordinates of a Lorentzian Line Congruence

Here, we offer a procedure for locating a Lorentzian line congruence from the Plucker coordinates. Therefore, from Equation (18), we have that $\langle \widehat{x}', \widehat{x} \rangle = \langle \widehat{x}, \widehat{\omega} \rangle = 0$. Thus, all higher derivatives can be gained in terms of $\widehat{\gamma}$. The dual coordinates of (\widehat{x}) can be situated in \mathbb{L}_f , as follows: we choose $\widehat{\mathbf{t}}$ relative to the set $\{\mathbf{s}; \widehat{\mathbf{r}}_1, \widehat{\mathbf{r}}_2, \widehat{\mathbf{r}}_3\}$ by its intercept distance φ^* , sustained on the $\mathbb{I}\mathbb{S}\mathbb{A}$ and the angle φ , sustained with respect to $\widehat{\mathbf{r}}_3$. We set the dual angles $\widehat{\vartheta} = \vartheta + \varepsilon\vartheta^*$, and $\widehat{\alpha} = \alpha + \varepsilon\alpha^*$, which recognize the positions of $\widehat{\mathbf{b}}$ and $\widehat{\mathbf{x}}$ along $\widehat{\mathbf{t}}$ (Figure 2). The signs are specified by the following: (ϑ, ϑ^*) , and (α, α^*) are in the right-hand Lorentzian screw rule with the thumb pointing along $\widehat{\mathbf{t}}$; the sense of $\widehat{\mathbf{t}}$ is such that $\vartheta \in \mathbb{R}$, and $\vartheta^* \geq 0$ are positioned with the thumb in the direction of the $\mathbb{I}\mathbb{S}\mathbb{A}$. Because $\widehat{\mathbf{x}}$ is a spacelike dual unit vector, we have:

$$\widehat{\mathbf{x}} = \sinh \widehat{\vartheta} \widehat{\mathbf{r}}_1 + \cosh \widehat{\vartheta} \widehat{\mathbf{m}}, \quad (31)$$

where $\widehat{\mathbf{m}} = \cos \widehat{\varphi} \widehat{\mathbf{r}}_2 + \sin \widehat{\varphi} \widehat{\mathbf{r}}_3$. Furthermore, we attain

$$\widehat{\mathbf{b}} = \cosh \widehat{\alpha} \widehat{\mathbf{r}}_1 + \sinh \widehat{\alpha} \widehat{\mathbf{m}}. \quad (32)$$

It is noticeable that the striction point \mathbf{s} is the origin of the induce Blaschke frame; that is, $\mathbf{s} = \mathbf{0}$ —see Figure 2.

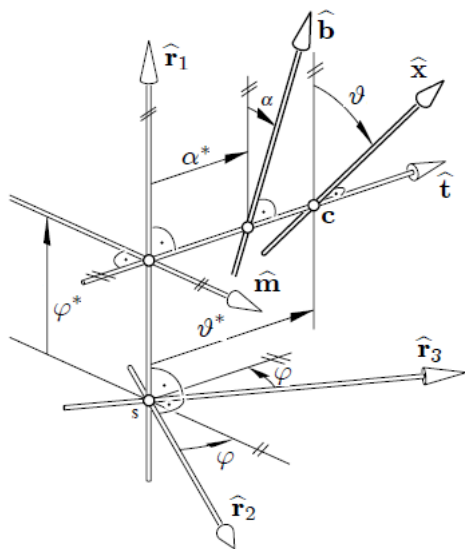


Figure 2. $\widehat{\mathbf{x}}$ and its Disteli-axis $\widehat{\mathbf{b}}$.

Considering the real and dual parts of $\widehat{\mathbf{x}}$ in Equation (31), we obtain:

$$\left. \begin{aligned} x_1 &= \sinh \vartheta, \quad x_1^* = \vartheta^* \cosh \vartheta, \\ x_2 &= \cosh \vartheta \cos \varphi, \quad x_2^* = \vartheta^* \sinh \vartheta \cos \varphi - \varphi^* \sin \varphi \cosh \vartheta, \\ x_3 &= \cosh \vartheta \sin \varphi, \quad x_3^* = \vartheta^* \sinh \vartheta \sin \varphi + \varphi^* \cos \varphi \cosh \vartheta. \end{aligned} \right\} \quad (33)$$

Let $\mathbf{a}(a_1, a_2, a_3)$ be a point on \hat{x} . Since $\mathbf{x}^* = a \times \mathbf{x}$, we obtain the linear equation system in $a_i (i = 1, 2, 3, \text{ and } a_{is} \text{ are the coordinates of } a)$:

$$\left. \begin{aligned} -a_2 \cosh \vartheta \sin \varphi + a_3 \cosh \vartheta \cos \varphi &= x_1^*, \\ -a_1 \cosh \vartheta \sin \varphi + a_3 \sinh \vartheta &= x_2^*, \\ a_1 \cosh \vartheta \cos \varphi - a_2 \sinh \vartheta &= x_3^*. \end{aligned} \right\} \tag{34}$$

The following skew symmetric matrix of coefficients of unknowns b_i is

$$\begin{pmatrix} 0 & -\cosh \vartheta \sin \varphi & \cosh \vartheta \cos \varphi \\ -\cosh \vartheta \sin \varphi & 0 & \sinh \vartheta \\ \cosh \vartheta \cos \varphi & -\sinh \vartheta & 0 \end{pmatrix},$$

and hence it has a rank of 2 with $\vartheta \neq 2\pi p$ (p is an integer). The rank of the augmented matrix

$$\begin{pmatrix} 0 & -\cosh \vartheta \sin \varphi & \cosh \vartheta \cos \varphi & x_1^* \\ -\cosh \vartheta \sin \varphi & 0 & \sinh \vartheta & x_2^* \\ \cosh \vartheta \cos \varphi & -\sinh \vartheta & 0 & x_3^* \end{pmatrix},$$

is also 2. There are therefore infinite solutions to this system, as shown by

$$\begin{aligned} -a_2 \sin \varphi + a_3 \cos \varphi &= \vartheta^* \\ a_2 &= (a_1 - \vartheta^*) \coth \vartheta \cos \varphi - \vartheta^* \sin \varphi, \\ a_3 &= (a_1 - \vartheta^*) \coth \vartheta \sin \varphi + \vartheta^* \cos \varphi. \end{aligned} \tag{35}$$

Since a_1 can be chosen arbitrarily, we can set $a_1 = \vartheta^*$. Therefore, Equation (35) becomes

$$a_1 = \vartheta^*, \quad a_2 = -\vartheta^* \sin \varphi, \quad a_3 = \vartheta^* \cos \varphi. \tag{36}$$

In this case, we have

$$\mathbf{a}(\varphi, \vartheta^*) = (\vartheta^*, -\vartheta^* \sin \varphi, \vartheta^* \cos \varphi) \tag{37}$$

which is the base or director surface of the Lorentzian line congruence. By Equations (33) and (37), the Lorentzian line congruence is

$$(\hat{x}) : \mathbf{y}(\varphi, \vartheta^*, t) = \begin{pmatrix} \vartheta^* + t \sinh \vartheta \\ -\vartheta^* \sin \varphi + t \cosh \vartheta \cos \varphi \\ \vartheta^* \cos \varphi + t \cosh \vartheta \sin \varphi \end{pmatrix}, \quad t \in \mathbb{R}. \tag{38}$$

The constants h, ϑ , and ϑ^* can control the shape of (\hat{x}) . If we let $\vartheta^* = h\varphi$ and φ as the movement parameter, then (\hat{x}) is a timelike ruled surface in \mathbb{L}_f -space. Hence, from Equations (37) and (38) and according to the shapes of its striction curves, the timelike ruled surface (\hat{x}) can be categorized into four types:

- (1) Timelike Archimedes with its striction curve is a timelike circular helix; for $h = 1, \vartheta^* = 0.5, \vartheta = 1.7, -2.5 \leq v \leq 2.5$, and $0 \leq \varphi \leq 2\pi$ (Figure 3).
- (2) Lorentzian unit sphere with its striction curve is a spacelike circle; for $h = 0, \vartheta^* = 1, \vartheta = 1.7, -2 \leq v \leq 2$, and $0 \leq \varphi \leq 2\pi$ (Figure 4).
- (3) Timelike helicoid with its striction curve is a timelike line; for $h = 1, \vartheta^* = 0, \vartheta = 1.7, -2 \leq v \leq 2$, and $0 \leq \varphi \leq 2\pi$ (Figure 5).
- (4) Timelike cone with its striction curve is a fixed point; for $h = \vartheta^* = 0, \vartheta = 1.7, -2 \leq v \leq 2$, and $0 \leq \varphi \leq 2\pi$ (Figure 6).

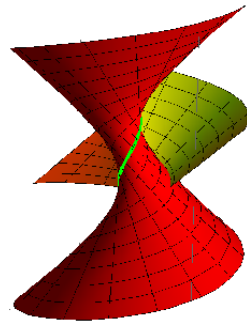


Figure 3. Timelike Archimedes.

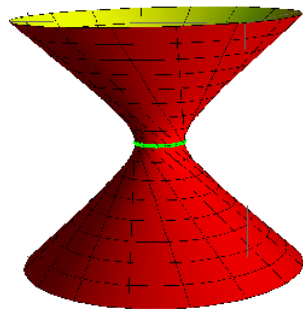


Figure 4. Lorentzian unit sphere.

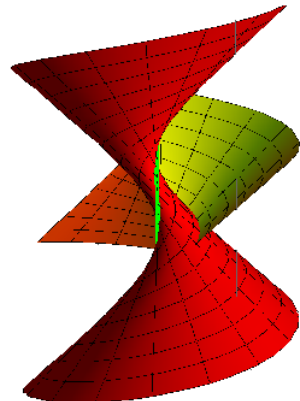


Figure 5. Timelike helicoid.

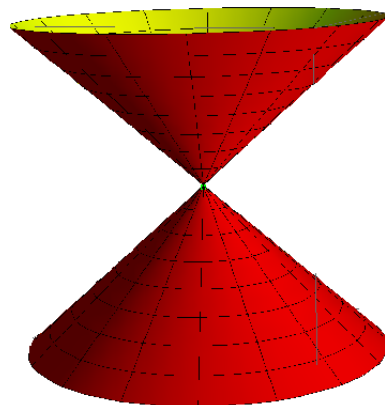


Figure 6. Timelike cone.

3.2. Lorentzian Inflection Line Congruence

We now define Lorentzian inflection line congruence, which is the spatial synonymous of the inflection circle in planar kinematic [1–3]. Then, from Equation (30), we have:

$$\widehat{\chi}(\widehat{v}) = \chi + \varepsilon\chi^* = 0 \Leftrightarrow \widehat{\kappa}(\widehat{v}) = 1. \quad (39)$$

Therefore, the spatial synonymous of the inflection circle in planar kinematic is located by (i) the Lorentzian line complex characterized by the inflection cone $c: \chi(s) = 0$, and (ii) the Lorentzian line complex characterized by the attached plane of lines $\pi: \chi^*(s) = 0$. All the set of spacelike lines \widehat{x} of the movable space \mathbb{L}_m and also in the plane satisfy $\pi: \chi^*(s) = 0$, initiating the Lorentzian inflection line congruence. Therefore, the Lorentzian inflection line congruence composed of a set of planes $\pi: \chi^*(s) = 0$, each of which is related with a direction of the inflection cone $c: \chi(s) = 0$.

Hence, we have attained the following theorem:

Theorem 1. *Through the movement $\mathbb{L}_m/\mathbb{L}_f$, consider a set of correlating spacelike lines of the movable timelike axode, such that each one of these lines has the analog of an inflection circle. Then, this set of spacelike lines forms a Lorentzian inflection line congruence which consists of common lines of the two Lorentzian line complexes $c: \chi(v) = 0$, and $\pi: \chi^*(v) = 0$.*

However, from Equation (30), we can also see that

$$\widehat{\chi} = \chi + \varepsilon(\Gamma - \mu\chi) = 0 \Leftrightarrow \tanh \widehat{\phi} = 0 \Leftrightarrow \phi = \phi^* = 0. \quad (40)$$

Now, the lines \widehat{x} , $\widehat{\mathbf{t}}$, and $\widehat{\mathbf{b}}$ specify the Blaschke frame and they are intersected at the striction point of the timelike ruled surface (\widehat{x}). From Equations (25) and (40) it could be assumed that the striction curve of (\widehat{x}) will have a tangent orthogonal to its creator, that is, $\frac{d\mathbf{c}}{du} \parallel \mathbf{g}$. In this case, (\widehat{x}) is a timelike binormal ruled surface with timelike striction curve. However, if we substitute $\widehat{\chi}(\widehat{v}) = 0$ into Equation (23), we obtain $\frac{d^2\widehat{x}}{d\widehat{v}^2} + \widehat{x} = \mathbf{0}$. The curve that satisfies this differential equation is a spacelike great dual circle on \mathbb{S}_{1f}^2 . For example, a spacelike great dual circle can be given as $\widehat{x}(\widehat{v}) = (0, \cos \widehat{v}, \sin \widehat{v})$. The tangent vector can be gained as $\widehat{\mathbf{t}}(\widehat{v}) = (0, -\sin \widehat{v}, \cos \widehat{v})$. Thus, $\widehat{\mathbf{g}}$ has the form $\widehat{\mathbf{g}}(\widehat{v}) = (1, 0, 0)$. Let $\mathbf{y}(x, y, z)$ be a point on $\widehat{x}(\widehat{v})$, then

$$(\widehat{x}) : \mathbf{y}(v, v^*, t) = (v^*, 0, 0) + t(0, \cos v, \sin v), \quad t \in \mathbb{R}, \quad (41)$$

which yields that:

$$x = v^*, \quad y = t \cos v, \quad z = t \sin v. \quad (42)$$

A relationship such as $f(v, v^*) = 0$ defines timelike ruled surface. Thus, we take $v^* = hv$, h indicating the pitch of \mathbb{L}_m/\mathbb{L} , and by eliminating v , and t , we obtain:

$$x = h \tan^{-1} \frac{z}{y},$$

This is a one-parameter family of timelike helicoidal surface of the 1st kind. If we let $h = 1$, $-2 \leq v \leq 2$, and $-1 \leq t \leq 1$, then a member of such family can be gained (Figure 7).

Theorem 2. *In the Minkowski 3-space \mathbb{E}_1^3 , any timelike helicoidal surface of 1st kind with timelike striction curve be included in Lorentzian inflection line congruence*

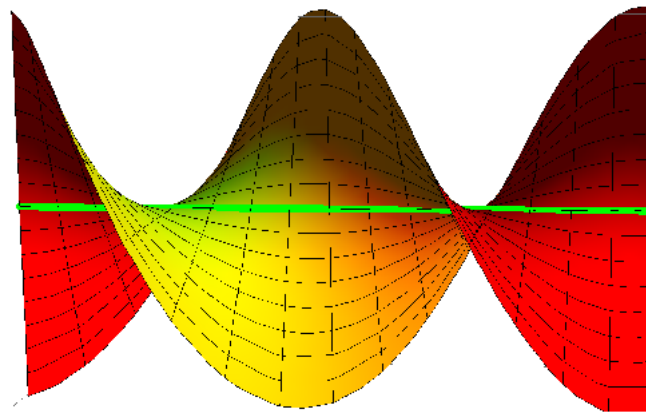


Figure 7. A timelike helicoid of 1st kind.

Analysis of the Lorentzian Inflection Line Congruence

In order to analyze the lines of the Lorentzian inflection line congruence (\hat{x}), from Equations (29), (31) and (40) we have

$$\hat{c} : \hat{\omega} \sinh 2\hat{\theta} - 2 \sin \hat{\varphi} = 0. \quad (43)$$

Equation (43) consists of the inflection trajectories in Lorentzian spherical kinematics (Compared with [1–3]). The real part of Equation (43) defines the Lorentzian inflection cone for the real Lorentzian spherical part of the movement $\mathbb{L}_m/\mathbb{L}_f$ and is given by:

$$c : -\omega \sinh 2\theta + 2 \sin \varphi = 0. \quad (44)$$

The intersection of this Lorentzian inflection cone with a real Lorentzian unit sphere fastened at the apex of the Lorentzian cone explains a spacelike spherical curve. There is a Lorentzian plane for each line, correlating with all orientations of a line of the Lorentzian inflection cone, provided by the dual part of Equation (43):

$$\pi : \omega^* \sinh 2\theta + 2\omega\theta^* \cosh 2\theta - 2\varphi^* \cos \varphi = 0. \quad (45)$$

Solving Equation (44) with respect to φ , we attain:

$$\sin \varphi = \left(\frac{\omega \sinh 2\theta}{2} \right), \text{ and } \cos \varphi = \pm \frac{1}{2} \sqrt{4 - \omega^2 \sinh^2 2\theta}. \quad (46)$$

Substituting Equation (46) into Equation (45), we find:

$$\pi : h \sinh 2\theta + 2\theta^* \cosh 2\theta \pm \frac{1}{2} \sqrt{4 - \omega^2 \sinh^2 2\theta} \varphi^* = 0. \quad (47)$$

Equation (47) is linear in the position coordinates φ^* and θ^* of the oriented line \hat{x} . Therefore, for a one-parameter Lorentzian spatial movement $\mathbb{L}_m/\mathbb{L}_f$, the spacelike lines in a given stationary direction in \mathbb{L}_m -space lie on a Lorentzian plane. In Figure 3, it is shown that the angle θ identifies the spacelike line \hat{x} ; hence, Equation (47) realizes two spacelike lines L^+ and L^- in the Lorentzian plane specified by $\hat{\mathbf{t}}$ and the ISA (L^+ , and L^- are identical to the inflection circle in planar kinematics). If the distance θ^* on the spacelike central normal $\hat{\mathbf{t}}$ from the ISA is accepted as the independent parameter, then Equation (47) becomes:

$$\pi : \theta^* = \mp \frac{\sqrt{4 - \omega^2 \sinh^2 2\theta}}{4 \cosh 2\theta} \varphi^* - \frac{1}{2} h \tan 2\theta. \quad (48)$$

We see that L^+ (or L^-) will alter its place if the parameter θ takes various values, but $\varphi = \text{constant}$. Meanwhile, the place of the Lorentzian plane π is altered if the parameter

φ of L^+ (or L^-) has several value, but $\vartheta = \text{constant}$. As a consequence, the set of all spacelike lines L^+ , and L^- realized by Equation (48) is the Lorentzian inflection line congruence for all values of (φ^*, ϑ^*) .

We can also examine the Lorentzian inflection line congruence as follows: if we choose the plus sign, then by substituting Equation (46) into the real part of Equation (31), we find:

$$\mathbf{x}(\vartheta) = \left(\sinh \vartheta, \frac{1}{2} \sqrt{4 - \omega^2 \sinh^2 2\vartheta} \cosh \vartheta, \frac{\omega \sinh 2\vartheta}{2} \cosh \vartheta \right), \tag{49}$$

where $-1 < 4 - \omega^2 \sinh^2 2\vartheta < 1$, and $\vartheta \in \mathbb{R}$. If we set $\varphi^* = h\varphi$, consider Equations (38), (46) and (49), then

$$(\hat{x}) : \mathbf{y}(\vartheta, \vartheta^*, t) = \begin{pmatrix} h \sin^{-1}(\frac{\omega}{2} \sinh 2\vartheta) + t \sinh \vartheta \\ -\vartheta^* \sin^{-1}(\frac{\omega}{2} \sinh 2\vartheta) + t \sqrt{1 - (\frac{\omega}{2} \sinh 2\vartheta)^2} \cosh \vartheta \\ \vartheta^* \sqrt{1 - (\frac{\omega}{2} \sinh 2\vartheta)^2} + t(\frac{\omega}{2} \sinh 2\vartheta) \cosh \vartheta \end{pmatrix}, t \in \mathbb{R}, \tag{50}$$

is the Lorentzian inflection line congruence. This congruence is composed of the timelike ruled surfaces $\mathbf{y}(\vartheta, \vartheta^*, v)$, $\vartheta = \vartheta^*$, $\mathbf{y}(\vartheta, \vartheta_0^*, v)$, $\vartheta_0^* = \text{constant}$, and $\mathbf{y}(\vartheta_0, \vartheta^*, v)$, $\vartheta_0 = \text{constant}$. Thus, according to Equations (49) and (50) we have the following:

- (1) Spacelike inflection spherical curve with timelike inflection ruled surface: for $\vartheta = \vartheta^*$, $h = 1$, $\omega = 0.5$, $-3 \leq \vartheta \leq 3$, and $-3 \leq t \leq 3$ (Figures 8 and 9).
- (2) Spacelike inflection spherical curve with timelike inflection ruled surface: for $\vartheta = \vartheta^*$, $h = 1$, $\omega = 1$, $-1.7 \leq \vartheta \leq 1.7$, and $-1.5 \leq t \leq 1.5$ (Figures 10 and 11).

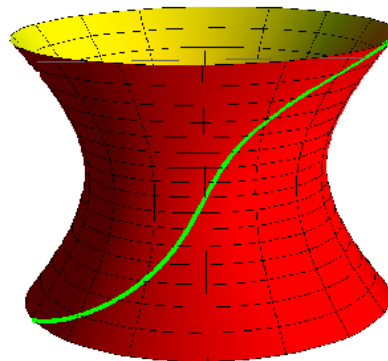


Figure 8. Inflection spacelike spherical curve (for $\omega = 0.5$, and $-3 \leq \vartheta \leq 3$).

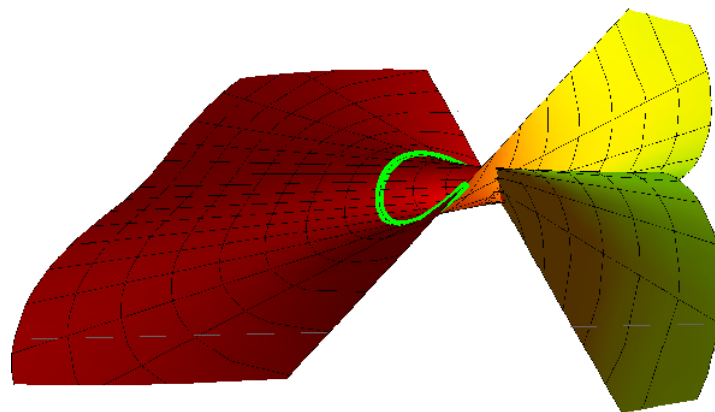


Figure 9. Timelike inflection ruled surface (for $\omega = 0.5$, and $-3 \leq \vartheta \leq 3$).

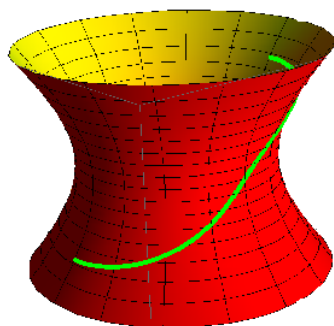


Figure 10. Inflection spacelike spherical curve (for $\vartheta = \vartheta^*$, $h = 1$, $\omega = 1$, $-1.7 \leq \vartheta \leq 1.7$, and $-1.5 \leq t \leq 1.5$).

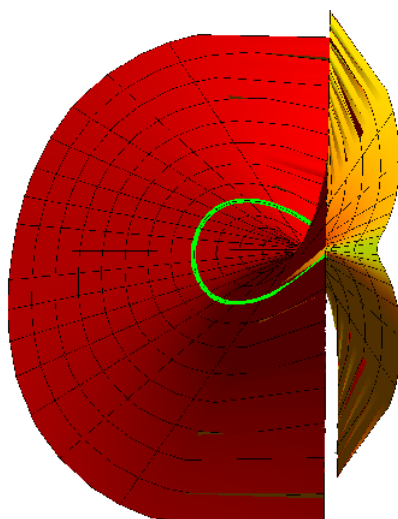


Figure 11. Timelike inflection ruled surface (for $\vartheta = \vartheta^*$, $h = 1$, $\omega = 1$, $-1.7 \leq \vartheta \leq 1.7$, and $-1.5 \leq t \leq 1.5$).

3.3. Euler–Savary Equation and Disteli Formulae

Disteli succeeded in discovering a curvature axis for the creating line of a ruled surface in 1914 [9], bringing the well-known planar Euler–Savary explanation to spatial kinematics. Calculating the dual spherical curvature of $\hat{\chi}(\hat{u})$ yields the Lorentzian Disteli equations as follows. The dual spherical radius of curvature $\hat{\psi}$ can be written by (see Figure 2):

$$\hat{\psi} = \hat{\vartheta} - \hat{\alpha} \Leftrightarrow \psi = \vartheta - \alpha, \quad \psi^* = \vartheta^* - \alpha^*. \tag{51}$$

Then, we have the identity

$$\hat{\chi}(\hat{v}) := \tanh \hat{\psi} = \tanh(\hat{\vartheta} - \hat{\alpha}). \tag{52}$$

From Equations (29) and (31), into Equation (52), we obtain

$$\tanh(\hat{\vartheta} - \hat{\alpha}) = \tanh \hat{\vartheta} - \frac{\sin \hat{\psi}}{\hat{\omega} \cosh^2 \hat{\vartheta}}.$$

After some algebraic manipulations, it can be reduced to:

$$\tanh \hat{\alpha} - \tanh \hat{\vartheta} = \frac{\hat{\omega}}{\sin \hat{\psi}}. \tag{53}$$

Equation (53) is a dual spherically Euler–Savary Equation (compare with [1–3]). Via the real and the dual parts, respectively, we have:

$$\tanh \alpha - \tanh \vartheta = \frac{\omega}{\sin \varphi}, \quad (54)$$

and

$$\varphi^* = [h - (\frac{\vartheta^*}{\sin^2 \vartheta} - \frac{\alpha^*}{\sin^2 \alpha}) \frac{\sin \varphi}{\omega}] \tan \varphi. \quad (55)$$

Equations (54) and (55) are new Disteli formulae in the one-parameter spatial movement; the first one gives the relationship through the places of the stationary line \hat{x} in the movable space \mathbb{L}_m and the Disteli-axis $\hat{\mathbf{b}}$. The second one distinguishes the distance from the line \hat{x} to the Disteli-axis $\hat{\mathbf{b}}$. At the end of this section, we can rederive the dual Euler–Savary Formula (10). Substituting $\hat{\vartheta} = \hat{\varphi}_m$, $\hat{\alpha} = \hat{\varphi}_f$, and $\varphi = \frac{\pi}{2}$, and $\varphi^* = 0$ into Equation (53), we gain, subsequent to simplifications, that

$$\tanh \hat{\varphi}_f - \tanh \hat{\varphi}_m = \hat{\omega}, \quad (56)$$

as claimed.

4. Conclusions

Based on E. Study's map, the instantaneous invariants of relative motion through two Lorentzian dual unit spheres are utilized to derive formulae for the velocity and acceleration of point trajectories (spacelike dual curve). The instantaneous invariants are related to the curvature and torsion expressions of this spacelike curve. The well-known inflection circle of spherical and planar kinematics is calculated in dual space. E. Study's map is then utilized to thoroughly study a Lorentzian inflection line congruence and its spatial equivalent. Finally, the axode invariants are used to provide new proofs of the Euler–Savary equation and the Disteli formulae.

The use of line geometry for investigating spatial kinematics in Minkowski 3-space \mathbb{E}_1^3 could be utilized to investigate specific problems and create novel applications. We shall be interested in the creation of timelike ruled surfaces as tooth margins for gears with skew axes in the future, as shown in [34,35].

Author Contributions: Conceptualization, A.A.A. and R.A.A.-B.; methodology, R.A.A.-B.; validation, A.A.A. and R.A.A.-B.; formal analysis, A.A.A. and R.A.A.-B.; investigation, R.A.A.-B.; resources, A.A.A. and R.A.A.-B.; data curation, A.A.A. and R.A.A.-B.; writing—original draft preparation, R.A.A.-B.; writing—review and editing, A.A.A.; visualization, R.A.A.-B.; supervision, R.A.A.-B.; project administration, A.A.A.; funding acquisition, A.A.A. All authors have read and agreed to the published version of the manuscript.

Funding: This research was funded by Princess Nourah bint Abdulrahman University Researchers Supporting Project number (PNURSP2023R337).

Data Availability Statement: Our manuscript has no associate data.

Acknowledgments: The authors would like to acknowledge the Princess Nourah bint Abdulrahman University Researchers Supporting Project number (PNURSP2023R337), Princess Nourah bint Abdulrahman University, Riyadh, Saudi Arabia

Conflicts of Interest: The authors declare that there is no conflict of interest regarding the publication of this paper.

References

1. Bottema, O.; Roth, B. *Theoretical Kinematics*; North-Holland Press: New York, NY, USA, 1979.
2. Karger, A.; Novak, J. *Space Kinematics and Lie Groups*; Gordon and Breach Science Publishers: New York, NY, USA, 1985.

3. Schaaf, A.; Ravani, B. Geometric continuity of ruled surfaces. *Comput. Aided Geom. Des.* **1998**, *15*, 289–310. [[CrossRef](#)]
4. Pottman, H.; Wallner, J. *Computational Line Geometry*; Springer: Berlin/Heidelberg, Germany, 2001.
5. Abdel-Baky, R.A.; Al-Solamy, F.R. A new geometrical approach to one-parameter spatial motion. *J. Eng. Math.* **2008**, *60*, 149–172. [[CrossRef](#)]
6. Abdel-Baky, R.A.; Al-Ghefari, R.A. On the one-parameter dual spherical motions. *Comp. Aided Geom. Des.* **2011**, *28*, 23–37. [[CrossRef](#)]
7. Özcan, B.; Senyurt, S. On some characterizations of ruled surface of a closed timelike curve in dual Lorentzian space. *Adv. Appl. Clifford Algebr.* **2012**, *22*, 939–953.
8. Al-Ghefari, R.A.; Abdel-Baky, R.A. Kinematic geometry of a line trajectory in spatial motion. *J. Mech. Sci. Technol.* **2015**, *29*, 3597–3608. [[CrossRef](#)]
9. Abdel-Baky, R.A. On the curvature theory of a line trajectory in spatial kinematics. *Commun. Korean Math. Soc.* **2019**, *34*, 333–349.
10. Aslan, M.C.; Sekerci, G.A. Dual curves associated with the Bonnet ruled surfaces. *Int. J. Geom. Methods Mod. Phys.* **2020**, *17*, 2050204. [[CrossRef](#)]
11. Alluhaibi, N. Ruled surfaces with constant Disteli-axis. *AIMS Math.* **2020**, *5*, 7678–7694. [[CrossRef](#)]
12. Abdel-Baky, R.A.; Tas, F. W-Line congruences. *Commun. Fac. Sci. Univ. Ank. Ser. A1 Math. Stat.* **2020**, *69*, 450–460. [[CrossRef](#)]
13. Abdel-Baky, R.A.; Naghi, M.F. A study on a line congruence as surface in the space of lines. *AIMS Math.* **2021**, *6*, 11109–11123. [[CrossRef](#)]
14. Gungor, M.A.; Ersoy, S.; Tosun, S. Dual Lorentzian spherical movements and dual Euler–Savary formula. *Eur. J. Mech. A/Solids* **2009**, *28*, 820–826. [[CrossRef](#)]
15. Alluhaibi, N.; Abdel-Baky, R.A. On the one-parameter Lorentzian spatial movements. *Int. J. Geom. Methods Mod. Phys.* **2019**, *16*, 1950197. [[CrossRef](#)]
16. Alluhaibi, N.A.; Abdel-Baky, R.A. On the kinematic-geometry of one-parameter Lorentzian spatial movement. *Int. J. Adv. Manuf. Technol.* **2022**, *121*, 7721–7731. [[CrossRef](#)]
17. Li, Y.; Alluhaibi, N.; Abdel-Baky, R.A. One-parameter Lorentzian dual spherical movements and invariants of the axodes. *Symmetry* **2022**, *14*, 1930. [[CrossRef](#)]
18. Li, Y.; Tuncer, O.O. On (contra)pedals and (anti)orthotomics of frontals in de Sitter 2-space. *Math. Meth. Appl. Sci.* **2023**, *1*, 1–15. [[CrossRef](#)]
19. Li, Y.; Erdogdu, M.; Yavuz, A. Differential Geometric Approach of Betchow-Da Rios Soliton Equation. *Hacet. J. Math. Stat.* **2022**, *1*, 1–12. [[CrossRef](#)]
20. Li, Y.; Abolarinwa, A.; Alkhalidi, A.; Ali, A. Some Inequalities of Hardy Type Related to Witten-Laplace Operator on Smooth Metric Measure Space. *Mathematics* **2022**, *10*, 4580. [[CrossRef](#)]
21. Li, Y.; Aldossary, M.T.; Abdel-Baky, R.A. Spacelike Circular Surfaces in Minkowski 3-Space. *Symmetry* **2023**, *15*, 173. [[CrossRef](#)]
22. Li, Y.; Chen, Z.; Nazra, S.H.; Abdel-Baky, R.A. Singularities for Timelike Developable Surfaces in Minkowski 3-Space. *Symmetry* **2023**, *15*, 277. [[CrossRef](#)]
23. Li, Y.; Alkhalidi, A.; Ali, A.; Abdel-Baky, R.A.; Saad, M.K. Investigation of ruled surfaces and their singularities according to Balschke frame in Euclidean 3-space. *AIMS Math.* **2023**, *8*, 13875–13888. [[CrossRef](#)]
24. Qian, Y.; Yu, D. Rates of approximation by neural network interpolation operators. *Appl. Math. Comput.* **2022**, *41*, 126781. [[CrossRef](#)]
25. Li, Y.; Eren, K.; Ayvaci, K.H.; Ersoy, S. The developable surfaces with pointwise v_1 -type Gauss map of Frenet type framed base curves in Euclidean 3-space. *AIMS Math.* **2023**, *8*, 2226–2239. [[CrossRef](#)]
26. Li, Y.; Abdel-Salam, A.A.; Saad, M.K. Primitivoids of curves in Minkowski plane. *AIMS Math.* **2023**, *8*, 2386–2406. [[CrossRef](#)]
27. Wang, G.S.; Guan, L.M. Neural network Interpolation operators of multivariate function. *J. Comput. Anal. Math.* **2023**, *431*, 115266. [[CrossRef](#)]
28. Li, Y.; Liu, S.; Wang, Z. Tangent developable and Darboux developables of framed curves. *Topol. Appl.* **2021**, *301*, 107526. [[CrossRef](#)]
29. Yang, Z.C.; Li, Y.; Erdogdu, M.; Zhu, Y.S. Evolving evolutoids and pedaloids from viewpoints of envelope and singularity theory in Minkowski plane. *J. Geom. Phys.* **2022**, *104513*, 1–23. [[CrossRef](#)]
30. Li, Y.; Wang, Z. Lightlike tangent developables in de Sitter 3-space. *J. Geom. Phys.* **2021**, *164*, 1–11. [[CrossRef](#)]
31. Li, Y.; Wang, Z.; Zhao, T. Geometric Algebra of Singular Ruled Surfaces. *Adv. Appl. Clifford Algebr.* **2021**, *31*, 1–19. [[CrossRef](#)]
32. Li, Y.; Abolarinwa, A.; Azami, S.; Ali, A. Yamabe constant evolution and monotonicity along the conformal Ricci flow. *AIMS Math.* **2022**, *7*, 12077–12090. [[CrossRef](#)]
33. Li, Y.; Ganguly, D. Kenmotsu Metric as Conformal η -Ricci Soliton. *Mediterr. J. Math.* **2023**, *20*, 193. [[CrossRef](#)]
34. Zhang, X.; Zhang, J.; Pang, B.; Zhao, X. An accurate prediction method of cutting forces in 5-axis flank milling of sculptured surface. *Int. J. Mach. Tools Manuf.* **2016**, *104*, 26–36. [[CrossRef](#)]
35. Calleja, A.; Bo, P.; Gonzalez, H.; Barton, M.; Norberto, L.; de Lacalle, L. Highly accurate 5-axis flank CNC machining with conical tools. *Int. J. Adv. Manuf. Technol.* **2018**, *97*, 1605–1615. [[CrossRef](#)]
36. Walfare, J. Curves and Surfaces in Minkowski Space. Ph.D. Thesis, K.U. Leuven, Faculty of Science, Leuven, Belgium, 1995.

37. López, R. Differential geometry of curves and surfaces in Lorentz-Minkowski space. *Int. Electron. J. Geom.* **2014**, *7*, 44–107. [[CrossRef](#)]
38. O’Neil, B. *Semi-Riemannian Geometry Geometry, with Applications to Relativity*; Academic Press: New York, NY, USA, 1983.

Disclaimer/Publisher’s Note: The statements, opinions and data contained in all publications are solely those of the individual author(s) and contributor(s) and not of MDPI and/or the editor(s). MDPI and/or the editor(s) disclaim responsibility for any injury to people or property resulting from any ideas, methods, instructions or products referred to in the content.